Available online www.ejaet.com

European Journal of Advances in Engineering and Technology, 2022, 9(2):17-25

Research Article ISSN: 2394 - 658X

A Model Reference Adaptive Flux scheme for a Sensorless Speed Control of an Induction Motor in a Perturbed Rotor State

Crescent Onyebuchi Omeje

Department of Electrical/Electronic Engineering, University of Port Harcourt, Rivers State Nigeria
*Corresponding author's E-mail: crescent.omeje@uniport.edu.ng

ABSTRACT

A sensorless speed control of an asynchronous machine has undoubtedly attractedgreat attention in academia and in the industry. The effects of an adjustable proportional integral (PI) controller on a sensor less speed control of a three-phase induction motor using the Model referencing adaptive flux system in a healthy rotor state and under a perturbed rotor condition was evaluated and presented in this paper. Model reference and adaptive system (MRAS) was applied for an accurate speed and rotor position detection for a three-phase induction motor drive under a perturbed rotor state. A very simple and an accurate gate signal generator for the pulse width modulator was applied. The measured speed from the motor was compared with the reference speed to produce an error in speed. This error was adjusted through the PI-controller and fed to a torque limiter through which the reference current needed for pulse width modulation of the inverter switching signals was produced. A significant deviation in steady state error in speed and torque was observed during a perturbed rotor state regardless of the adjustment with the PI-controller. The simulation results obtained have clearly shown that the settling time of oscillation in speed and torque is much reduced with obvious decrease in the ripple values as the motor operates in a safe rotor condition and this also reduces the risk of downtime problem. The vector control method was applied with all the mathematical modeling simulated in MATLAB/SIMULINK 2017 version.

Key words: Induction Motor, Model reference adaptive system, Pulse width generator, Voltage Source Inverter, Speedand torque control

INTRODUCTION

A sensorless vector control of squirrel cage induction motor has become very prevalent in the industry due to its reliability, economic viability and provable maintenance culture [1-2]. A sensorless vector control of an asynchronous machine essentially implies the vector control of a non-synchronous speed operated a.c machines such as the squirrel cage and wound rotor induction motors without an embedded speed sensor [3-4]. The elimination of the rotor speed sensor without affecting its performance is a major trend in advanced drives control system [5]. The obvious advantages associated with sensorless speed control of ac drives are not limited to reduced hardware complexity, cost minimization, improved noise immunity, less maintenance requirements and high robustness. An indirect vector control of an induction motor requires precise speed information that incorporates a speed sensor on the motor shaft for accurate speed measurement. However, the speed sensor increases the system complexity, cost of purchase and requires a connection cable between the control system and the motor [6]. To avert these defects, a sensorless speed control of an induction motor has recently been invoked with different methods of estimating the rotor speed and its position. The model reference adaptive system (MRAS) is gaining popularity due to its simplicity and accuracy. The MRAS approach has the advantages of using two independent machine models for estimating the same state variable. The estimator that does not contain the speed to be computed is considered as a reference model whereas that which contains the estimated variable is regarded as an adjustable model [7]. In low speed region for a comprehensive or complete drive strategy, high frequency signals are usually injected to extract the position and speed signals [8-9]. This is primarily to achieve a perfect speed control at standstill within the low speed regions. Though this method has its inherent disadvantage of introducing a high frequency noise to the system. Kim et al estimated the rotor speed using Extended-Kalman Filter [10]. However, Kalman Filter is relatively complicated and needs more powerful microprocessors [11]. The use of state observers to estimate rotor speed and position have as well been considered in different methods such as the sliding mode observers and Unscented Kalman filters [12-14]. The output signals in these methods are equivalent with the actual state of the system though it presents very complex computations. Other sensorless control scheme includes a back emf method which has a limitation of sensitivity to stator resistance mismatch and noise during a low speed operation [15-17]. The concepts of the Model reference adaptive system (MRAS) were proposed in [18-20]. The simplicity and excellent dynamic performanceof this method makes it very efficient for accurate speed and position sensing of an induction motor drive.

Derived Model Equations of an Induction Motor

The model equations of a squirrel-cage induction motor expressed as a set of differential equations for stator current and rotor flux components as compiled in [21-23] are presented in (1)-(4).

$$\frac{d(i_{ds}^s)}{dt} = \frac{-(R_s L_r^2 + R_r L_m^2)}{\sigma L_s L_r^2} i_{ds}^s + \frac{R_r L_m}{\sigma L_s L_r^2} \psi_{dr}^s + \frac{L_m \omega_r}{\sigma L_s L_r} \psi_{qr}^s + \frac{1}{\sigma L_s} V_{ds}^s . \quad (1)$$

$$\frac{d(i_{qs}^s)}{dt} = \frac{-(R_s L_r^2 + R_r L_m^2)}{\sigma L_s L_r^2} i_{qs}^s + \frac{R_r L_m}{\sigma L_s L_r^2} \psi_{qr}^s - \frac{L_m \omega_r}{\sigma L_s L_r} \psi_{dr}^s + \frac{1}{\sigma L_s} V_{qs}^s . \quad (2)$$

$$\frac{d(\psi_{dr}^s)}{dt} = -\frac{R_r}{L_r}\psi_{dr}^s - \omega_r \psi_{qr}^s + \frac{L_m R_r}{L_r} i_{ds}^s \quad (3)$$

$$\frac{d(\psi_{qr}^s)}{dt} = -\frac{R_r}{L_r}\psi_{qr}^s + \omega_r \psi_{dr}^s + \frac{L_m R_r}{L_r} i_{qs}^s . \quad (4)$$

Re-expressing (1)-(4) in state space gives rise to (5) as shown:

$$\frac{d}{dt}\begin{bmatrix} i_{ds}^s \\ i_{qs}^s \\ \psi_{dr}^s \\ \psi_{qr}^s \end{bmatrix} = A \begin{bmatrix} i_{ds}^s \\ i_{qs}^s \\ \psi_{dr}^s \\ \psi_{qr}^s \end{bmatrix} + B \begin{bmatrix} V_{ds}^s \\ V_{qs}^s \\ 0 \\ 0 \end{bmatrix} . \quad (5)$$

Where $A = \begin{bmatrix} \frac{-(R_s L_r^2 + R_r L_m^2)}{\sigma L_s L_r^2} & 0 & \frac{R_r L_m}{\sigma L_s L_r^2} & \frac{L_m \omega_r}{\sigma L_s L_r} \\ 0 & \frac{-(R_s L_r^2 + R_r L_m^2)}{\sigma L_s L_r^2} & \frac{-L_m \omega_r}{\sigma L_s L_r} & \frac{R_r L_m}{\sigma L_s L_r^2} \\ \frac{L_m R_r}{L_r} & 0 & -\frac{R_r}{L_r} & -\omega_r \\ 0 & \frac{L_m R_r}{L_r} & \omega_r & -\frac{R_r}{L_r} \end{bmatrix}$ and $B = \begin{bmatrix} \frac{1}{\sigma L_s} & 0 & 0 & 0 \\ 0 & \frac{1}{\sigma L_s} & 0 & 0 \\ 0 & 0 & 0 & 0 \\ 0 & 0 & 0 & 0 \end{bmatrix}$

Basic equations of rotor flux based-MRAS are represented in (6) and (7) by modifying (5).

A modified Stator Reference Model equation in state space is given in (6):

$$\frac{d}{dt}\begin{bmatrix} \psi_{dr}^s \\ \psi_{qr}^s \end{bmatrix} = \frac{L_r}{L_m}\left[\begin{bmatrix} V_{ds}^s \\ V_{qs}^s \end{bmatrix} - \begin{bmatrix} (R_s + \sigma L_s S) & 0 \\ 0 & (R_s + \sigma L_s S) \end{bmatrix}\begin{bmatrix} i_{ds}^s \\ i_{qs}^s \end{bmatrix}\right] . \quad (6)$$

A modified Rotor Adaptive Model equation in state space is given in (7):

$$\frac{d}{dt}\begin{bmatrix} \widetilde{\psi}_{dr}^s \\ \widetilde{\psi}_{qr}^s \end{bmatrix} = \begin{bmatrix} \frac{-R_r}{L_r} & -\omega_r \\ \omega_r & \frac{-R_r}{L_r} \end{bmatrix}\begin{bmatrix} \widetilde{\psi}_{dr}^s \\ \widetilde{\psi}_{qr}^s \end{bmatrix} + \frac{R_r L_m}{L_r}\begin{bmatrix} i_{ds}^s \\ i_{qs}^s \end{bmatrix} . \quad (7)$$

Where $\sigma = 1 - \frac{L_m^2}{L_s L_r}$ represent the leakage inductance coefficient and S = $\frac{d}{dt}$. The outputs of (6) and (7) are integrated to produce the fluxes used in the analysis of the estimated speed. A perturbed rotor condition may occur as a result of a broken rotor or as a result of cracked end ring fault. A broken rotor bar was assumed. This condition can be simulated by increasing the rotor resistance above the rated value. The more the resistance is increased the more severity is added to the machine [24-27]. If an increased bar resistance of R_b value is injected into the rotor during its perturbed condition, then R_r in (1)-(4) and (7) changes to $R_r + R_b$ as shown in (8)-(12).

$$\frac{d(i_{ds}^s)}{dt} = \frac{-(R_s L_r^2 + (R_r + R_b) L_m^2)}{\sigma L_s L_r^2} i_{ds}^s + \frac{(R_r + R_b) L_m}{\sigma L_s L_r^2} \psi_{dr}^s + \frac{L_m \omega_r}{\sigma L_s L_r} \psi_{qr}^s + \frac{1}{\sigma L_s} V_{ds}^s . \quad (8)$$

$$\frac{d(i_{qs}^{s})}{dt} = \frac{-(R_s L_r^2 + (R_r + R_b)L_m^2)}{\sigma L_s L_r^2} i_{qs}^{s} + \frac{(R_r + R_b)L_m}{\sigma L_s L_r^2}\psi_{qr}^{s} - \frac{L_m \omega_r}{\sigma L_s L_r}\psi_{dr}^{s} + \frac{1}{\sigma L_s} V_{qs}^{s}. \quad (9)$$

$$\frac{d(\psi_{dr}^{s})}{dt} = -\left(\frac{R_r + R_b}{L_r}\right)\psi_{dr}^{s} - \omega_r \psi_{qr}^{s} + \frac{L_m (R_r + R_b)}{L_r} i_{ds}^{s}. \quad (10)$$

$$\frac{d\left(\psi_{qr}^{s}\right)}{dt} = -\left(\frac{R_r + R_b}{L_r}\right)\psi_{qr}^{s} + \omega_r \psi_{dr}^{s} + \frac{L_m (R_r + R_b)}{L_r} i_{qs}^{s}. \quad (11)$$

$$\frac{d}{dt}\begin{bmatrix}\widetilde{\psi_{dr}^{s}} \\ \widetilde{\psi_{qr}^{s}}\end{bmatrix} = \begin{bmatrix} -\left(\frac{R_r + R_b}{L_r}\right) & -\omega_r \\ \omega_r & -\left(\frac{R_r + R_b}{L_r}\right)\end{bmatrix}\begin{bmatrix}\widetilde{\psi_{dr}^{s}} \\ \widetilde{\psi_{qr}^{s}}\end{bmatrix} + \frac{L_m (R_r + R_b)}{L_r}\begin{bmatrix} i_{ds}^{s} \\ i_{qs}^{s}\end{bmatrix}. \quad (12)$$

The electromagnetic torque in terms of electrical variables is presented in (13).

$$T_{em} = \frac{3}{2} \times \frac{P}{2} \times \left(\lambda_{dr}^{s} i_{qs} - \lambda_{qr}^{s} i_{ds}\right). \quad (13)$$

The electromagnetic torque in terms of mechanical variables is obtained from (14).

$$T_{em} = B\omega_r + J\frac{d\omega_r}{dt} + T_{Load}. \quad (14)$$

$$\frac{d\omega_r}{dt} = \frac{1}{J}(T_{em} - T_{Load} - B\omega_r) \quad (15)$$

$$\omega_r = \int (d\omega_r)\, dt \quad (16)$$

$$\theta_r = \int (\omega_r) \quad (17)$$

Where J = moment of inertia of the mechanical axis (Kg-m^2), T_{Load} = applied load torque (Nm), ω_m = mechanical speed of the machine (Rad/Sec), B = coefficient of viscous friction (Nms^2). In equation (13), the torque is proportional to the stator quadrature axis current i_{qs}. If the q-axis flux component λ_{qr}^{s} becomes zero and the d-axis flux component λ_{dr}^{s} is aligned with the rotor flux axis at constant value, then equation (13) is linearized to form equation (18). This equation is similar to that of a separately excited dc motor and therefore forms the basic philosophy of the vector control of an induction motor.

$$T_{em} = \frac{3}{2} \times \frac{P}{2} \times \left(\lambda_{dr}^{s} i_{qs}\right). \quad (18)$$

The non-linear differential equation that describes the dynamic performance of an ideal symmetrical induction machine in the arbitrary reference frame with the dq-axis voltage is presented in equation (19).

$$\begin{bmatrix} V_{qs} \\ V_{ds} \\ 0 \\ 0 \end{bmatrix} = \begin{bmatrix} (R_s + L_s p) & \omega L_s & L_m p & \omega L_m \\ -\omega L_s & (R_s + L_s p) & -\omega L_m & L_m p \\ L_m p & (\omega - \omega_r) L_m & (R_r' + L_r' p) & (\omega - \omega_r) L_r' \\ -(\omega - \omega_r) L_m & L_m p & -(\omega - \omega_r) L_r' & (R_r' + L_r' p) \end{bmatrix} \times \begin{bmatrix} i_{qs} \\ i_{ds} \\ i_{qr}' \\ i_{dr}' \end{bmatrix} \quad (19)$$

Where: $L_s = L_{Ls} + L_m$ (20)

$$L_r = L_{Lr} + L_m \quad (21)$$

$$p = \frac{d}{dt} \quad (22)$$

A Sensorless Vector Control System of an Induction Motor with MRAS

In vector control method, flux and current are separated to linearly control the output torque of an induction motor. Vector control requires precise information of the angular position of the rotor flux. Model referencing adaptive system (MRAS) is designed to estimate the rotor speed and position. The aim is to decrease the speed and torque fluctuations of the asynchronous machine during sudden load changes. Conventionally, two independent machine models of different structures are usually considered in the model reference adaptive approach to estimate the same state variables (back emf, rotor flux, reactive power and current) based on different sets of input variables. The error obtained from the actual and estimated output is fed to the adaptation set up through a PI-controller which outputs the estimated rotor speed. This estimated speed is processed by the integrator to obtain the estimated rotor position θ_{est}. The estimated speed is tuned through a PI-controller with the adjustable model until the speed error is reduced to zero.At this condition, the estimated speed is made equal to the actual speed. Fig. 1 represents a block diagram of the MRAS which is achieved with the aid of equations (23) to (26).

$$i_{ds} = \frac{1}{L_m}\left[\lambda_{dr} + \omega_r T_r \lambda_{qr} + T_r P \lambda_{dr}\right] \quad (23)$$

$$i_{qs} = \frac{1}{L_m}\left[\lambda_{qr} - \omega_r T_r \lambda_{dr} + T_r P \lambda_{qr}\right] \quad (24)$$

The estimated stator current equation is given by equations (28) and (29).

$$\widehat{i_{ds}} = \frac{1}{L_m}\left[\lambda_{dr} + \widehat{\omega_r} T_r \lambda_{qr} + T_r P \lambda_{dr}\right] \quad (25)$$

$$\widehat{i_{qs}} = \frac{1}{L_m}\left[\lambda_{qr} - \widehat{\omega_r} T_r \lambda_{dr} + T_r P \lambda_{qr}\right] \quad (26)$$

The circumflex ^ is used to distinguish the state variables of the adjustable model from the reference model. Error in rotor speed is obtained from equations (27) and (28).

$$(i_{ds} - \widehat{i_{ds}})\lambda_{qr} + (\widehat{i_{qs}} - i_{qs})\lambda_{dr} = \frac{T_r}{L_m}(\lambda_{qr}^2 - \lambda_{dr}^2)[\omega_r - \widehat{\omega_r}] \quad (27)$$

$$[\omega_r - \widehat{\omega_r}] = \left(\frac{(i_{ds} - \widehat{i_{ds}})\lambda_{qr} + (\widehat{i_{qs}} - i_{qs})\lambda_{dr}}{K}\right) \quad (28)$$

Where $K = \frac{T_r}{L_m}(\lambda_{qr}^2 - \lambda_{dr}^2)$ (29)

The complete equation for the estimated error in rotor speed $\omega_r - \widehat{\omega_r}$ with PI-controller is given by equation (30).

$$\omega_r - \widehat{\omega_r} = \frac{1}{K}\left[K_p\left((i_{ds} - \widehat{i_{ds}})\lambda_{qr} - (i_{qs} - \widehat{i_{qs}})\lambda_{dr}\right) + K_i \int \left((i_{ds} - \widehat{i_{ds}})\lambda_{qr} - (i_{qs} - \widehat{i_{qs}})\lambda_{dr}\right)\right] \quad (30)$$

The estimated electrical rotor position θ_{est} is obtained from equation (31).

$$\theta_{est} = \int_0^t (\widehat{\omega_r})\, dt \quad (31)$$

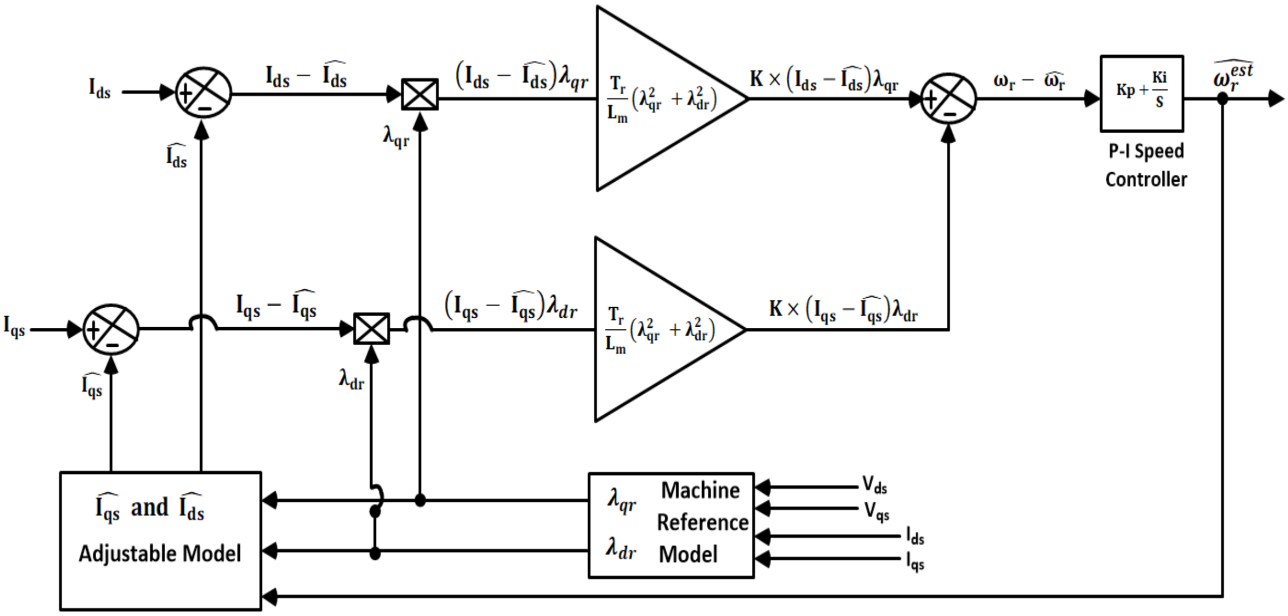

Fig. 1 Block Diagram of MRAS Control

The sensorless speed control scheme of low cost a.c induction machine drive is shown in Fig. 2. It incorporates the speed controller which receives the error signal from the reference speed ω_{ref} and the actual observed speed from the motor shaft and processes it to eliminate the steady state error in speed. The PI speed controller generates the torque signal command (T_e^*) which is restricted to an upper and lower limit of +75Nm and -75Nm through a torque limiter. This process helps in producing a reference torque needed for comparing the actual motor output torque T_e. The quadrature axis current under vector control i_{qs}^s is obtained from equation (18) using the torque divisor $\left(\frac{1}{\frac{3P}{22}\lambda_{dr}^s}\right)$ as shown in Fig. 2. The stator currents are transformed to the equivalent abc form using the inverse Parks transformation. The resultant three phase currents of pure sinusoidal waveforms are applied as reference waveforms in the pulsewidth modulator for the generation of gate signals that trigger the eight switches of the multi-level phase voltage source inverter that drives the induction motor. The overall control block diagram is shown in Fig. 2 while the algorithm for the MRAS is summarized in the flow chart shown in Fig. 3.

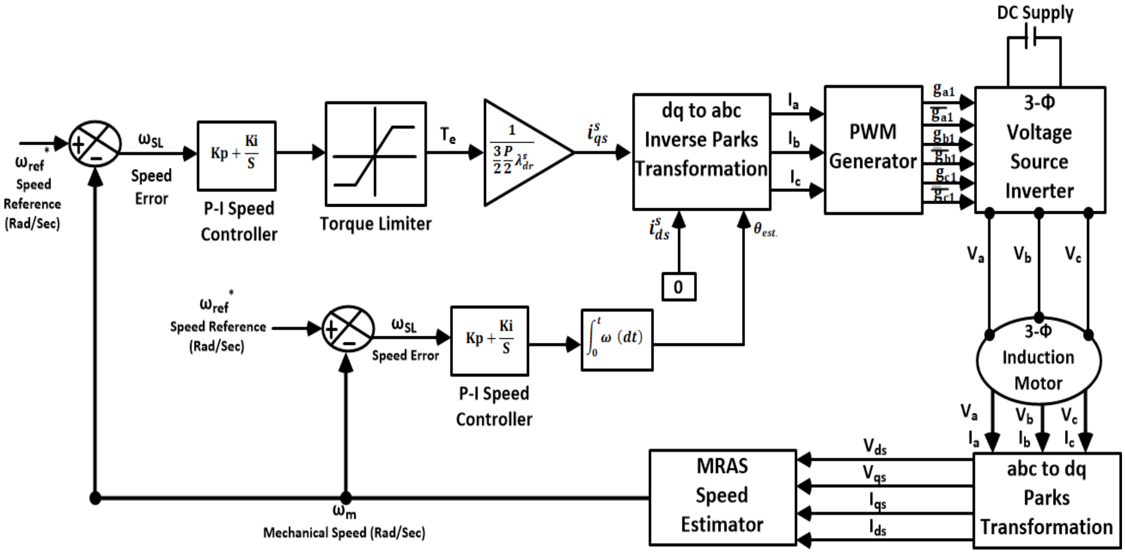

Fig. 2 Control Block Diagram of a Sensorless Vector Control of an Induction Motor

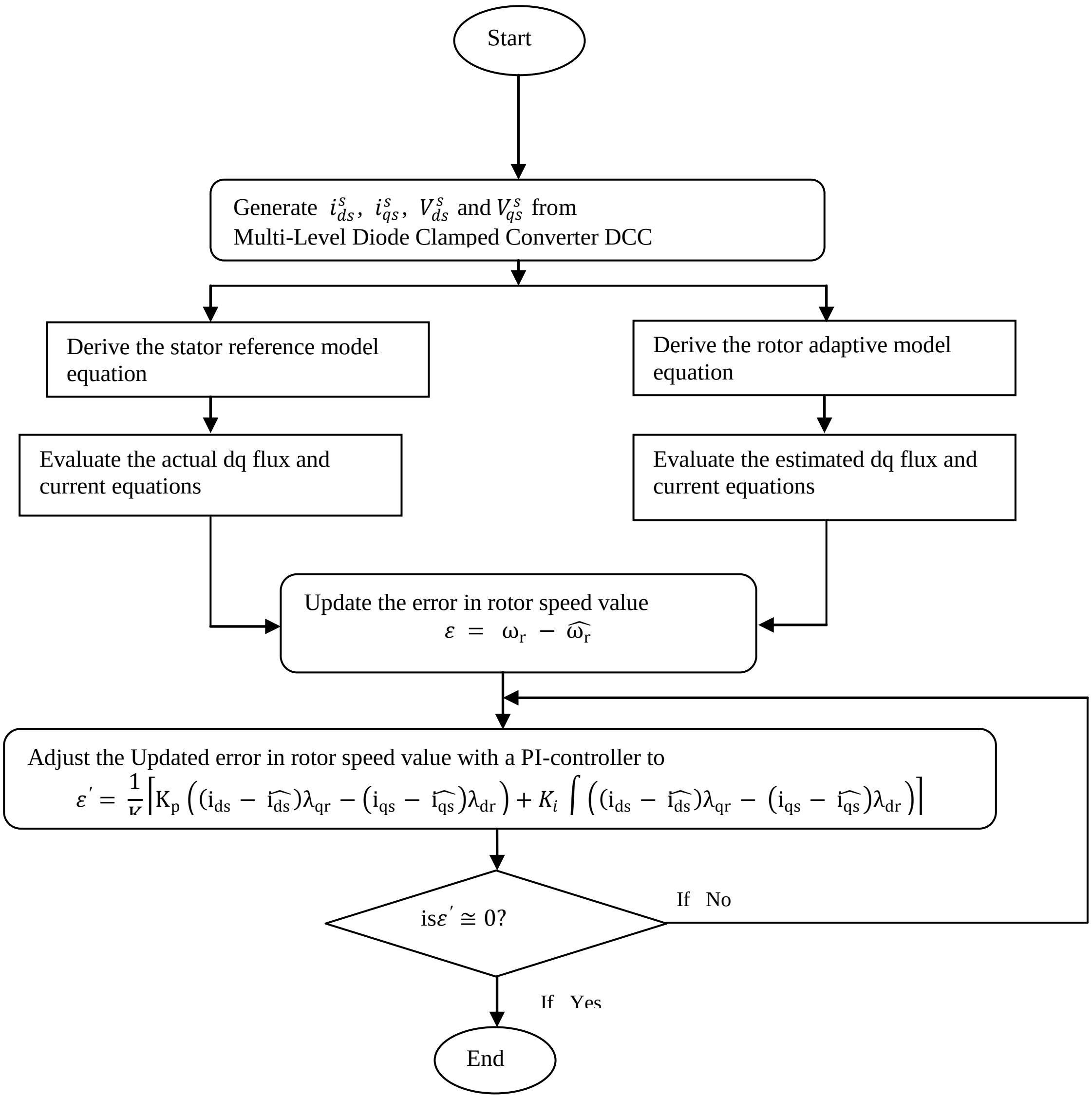

Fig. 3 A Flow Chart for the speed control

SIMULATION RESULTS AND DISCUSSION

Simulation was carried out on the induction machine during a healthy and perturbed rotor state using the machine parameters presented in table 1. Fig. 4 and 5 represents the inverter output voltages supplied to the stator terminal. A reduced percentage value of 3.06% was observed in Fig. 5 as against 30.04% obtained in Fig. 4. The dq-axes stator current and flux linkages were presented in Figs. 6 and 7. A sudden change in their values at a simulation period of 1.25 second is a consequence of a sudden change in applied load torque. The dynamic responses of the control system due to step changes in the speed were evaluated by subjecting the motor to a step decrease of 198.5 rad/sec to 165.5 rad/sec. It is clearly shown in Fig. 8 that the estimated speed and adaptive speed closely tracked the reference speed prior to the drop in speed under a healthy rotor condition with a nearly zero steady state error after the adjustment with a PI-controller. In Fig. 9, it is observed that the estimated speed and the adaptive speed deviated from the reference speed with a significant steady state error prior to the drop in reference speed under a perturbed rotor condition regardless of the adjustment made with a PI-controller. More transients (ripples) were also obtained with a longer settling time of 0.55second. In Figs. 10 and 11, plots of torque against time under a healthy and perturbed state were presented. The comparison drawn from the two plots showed that under a healthy rotor state, the torque developed by the machine settled and attained steady state faster at a simulation time of 0.25sec for the estimated torque and 0.3second for the adaptive torque as opposed to 0.35 second for the estimated torque and 0.55 second for the adaptive torque in a perturbed rotor state. Similarly, a close observation showed that the magnitude of torque ripples is more pronounced in Fig. 11 than in Fig. 10. It is therefore unsafe to run the machine over a prolonged time under this condition.The plot of rotor position is shown in Fig. 12. It is observed that the rotor angular position for the MRAS within the plot is ahead of the rotor angular position for the model with the speed sensor. In Fig. 13, a plot of the rotor angle against time for a perturbed rotor state was presented. The plot showeda wider deviation between the rotor angular position with MRAS and speed sensor in a perturbed rotor state. This concept actually accounts for the MRAS restoring to steady state at a faster rate than the model with the speed sensor. The comparative behaviour of the machine proved that introduction of severity such as end ring fault and broken rotor bar generates higher speed and torque ripples in the rotor axis.

Table -1 Simulation Parameters for 20 HP Induction Motor

Machine Parameters	**Values of Parameters**
Rated Power P(HP)	20
Rated Line-Line Stator Voltage V_{LL} **(Volts)**	400
Stator Resistance R_s**(Ω)**	22
Rotor Resistance R_r**(Ω)**	26
Rotor Bar Resistance R_b**(Ω)**	40
Stator Leakage Inductance Ls **(H)**	0.8264
Rotor Leakage Inductance Lr **(H)**	0.8264
Magnetizing Inductance Lm **(H)**	0.7844
Number of Pole	2
Frequency F **(H_Z)**	50
Synchronous Speed Ns **(Rpm)**	3000 (314.2 Rad/Sec.)
Load Torque Applied To Mechanical Axis T_{load} **(Nm)**	95.5
Motor Inertia J **($Kg\text{-}M^2$)**	0.025

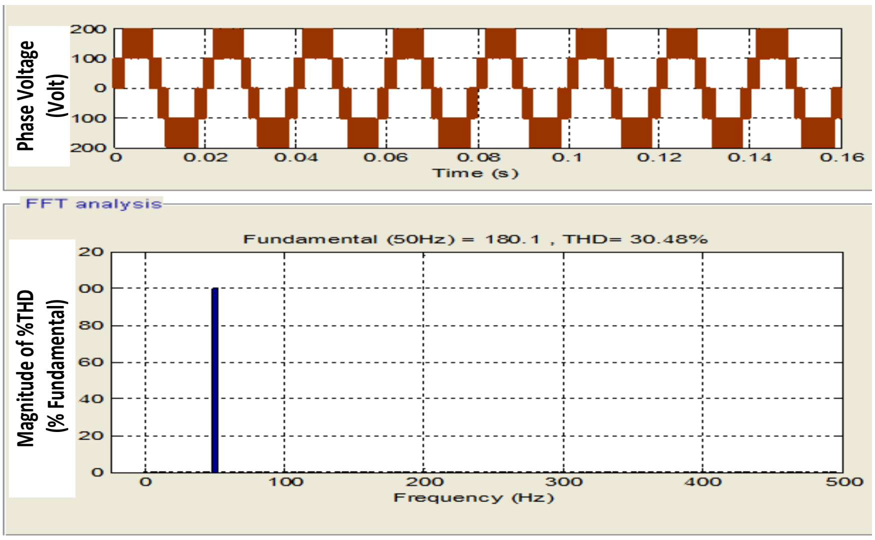

Fig. 4 A Plot of Phase A Five-level Inverter Output Voltage

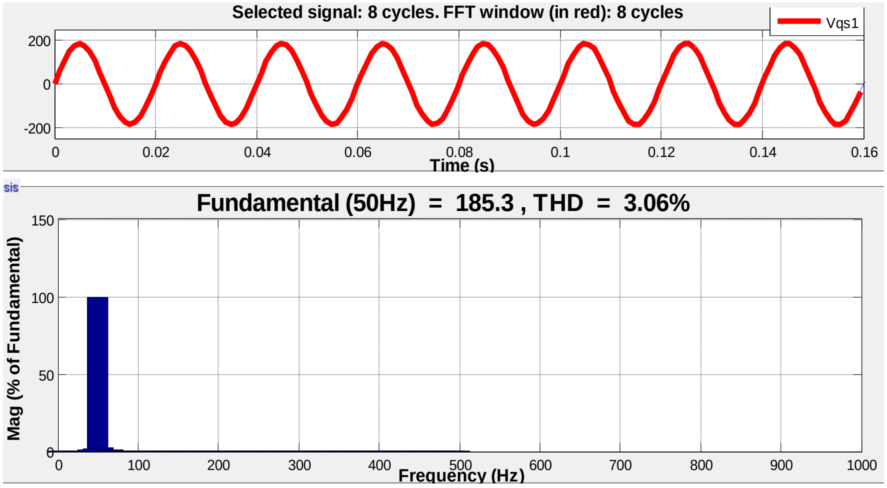

Fig. 5 A Plot of Inverter Filtered output Voltage

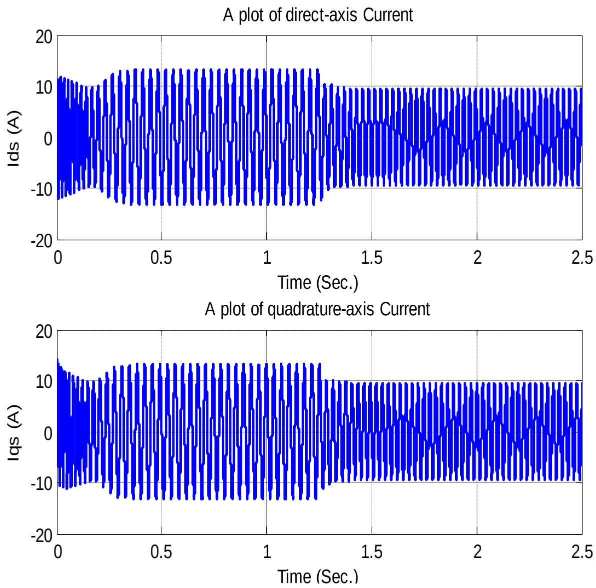

Fig. 6 dq-axes stator current

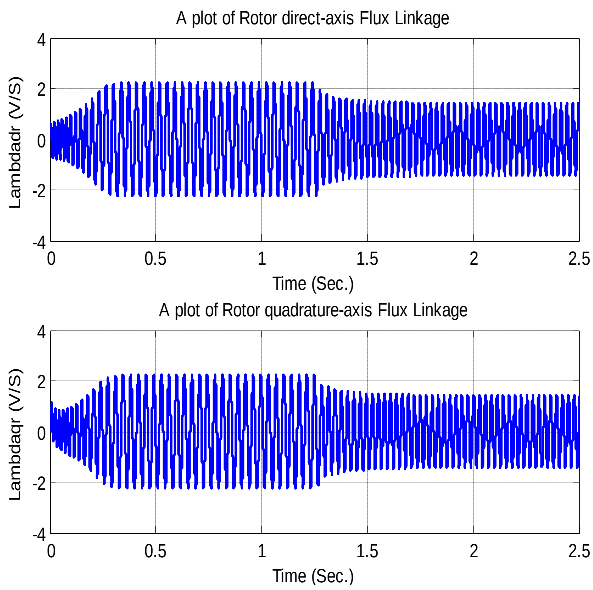

Fig. 7 dq-axes flux linkage

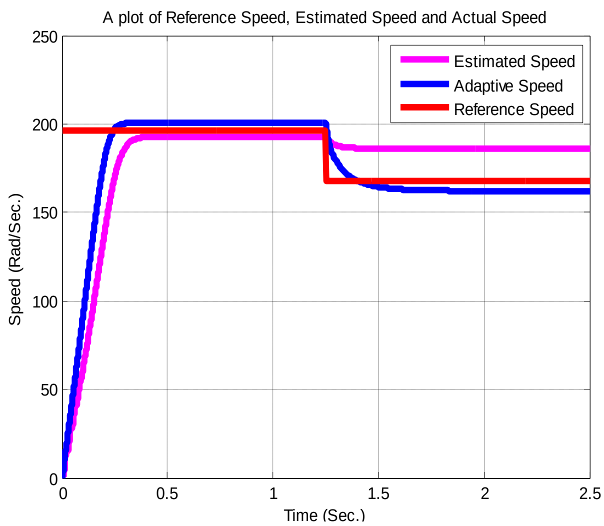

Fig. 8 A Plot of Estimated, Adaptive & Reference Speed

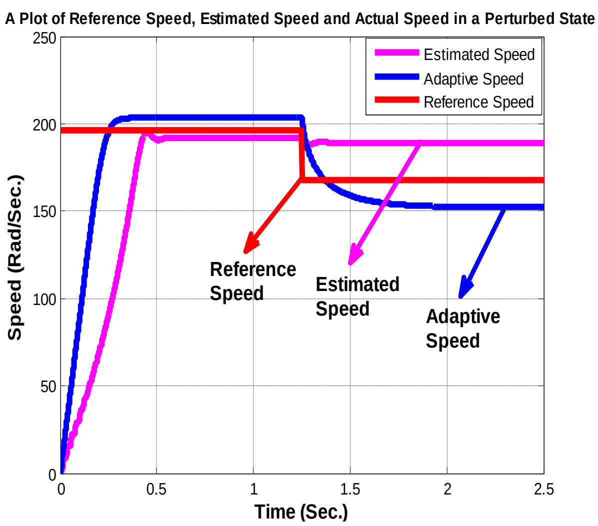

Fig. 9 A Plot of Estimated, Adaptive & Reference Speed in a perturbed state

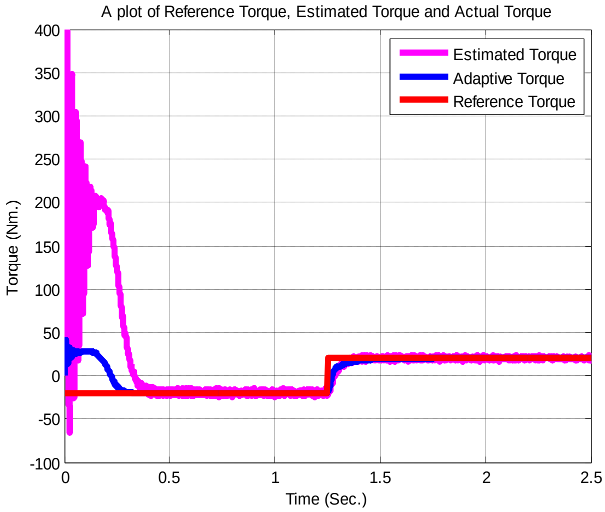

Fig. 10 A Plot of Estimated, Adaptive & Reference Torque

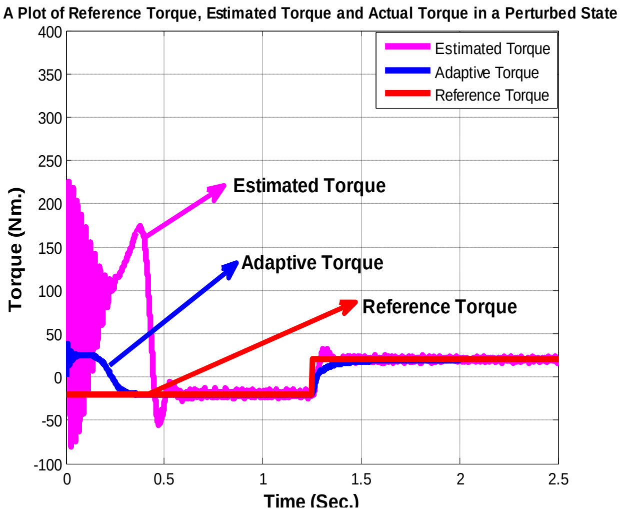

Fig. 11 A Plot of Estimated, Adaptive & Reference Torque under a perturbed state

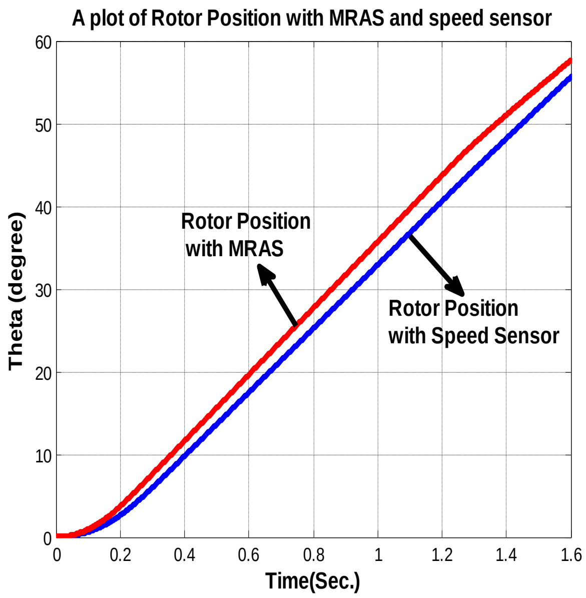

Fig. 12 A Plot of Rotor Angle against Time

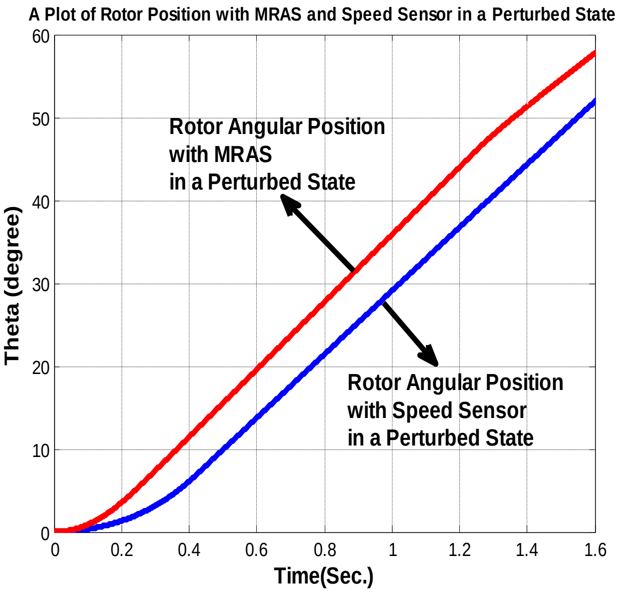

Fig. 13A Plot of Rotor Angle against Time under a perturbed state

CONCLUSION

The performance of a sensorless speed control of induction motor using MRAS in a perturbed rotor state was achieved. The results obtained showed a pronounced deviation in the rotor angular position under a perturbed state. The steady state error in speed and torque was very minimal while an excellent performance was achieved with MRAS in a healthy rotor state. This is proven by the high quality speed and torque responses of the machine with MRAS during transient and steady state as earlier demonstrated in the settling time of the machine speed and torque.

REFERENCE

[1]. J. Guzinski, H Abu-Rub. Speed Sensorless Induction motor drive with predictive current controller. IEEE Transaction on Industrial Electronics. 2013, 60(2), 699-709.

[2]. R. Purushottama, N. Jayaram, R. Shelsar. Sensorless vector control of induction machine using MRAS techniques. International Conference oncircuits' power and computing technologies. Nagercoil India. 2013, 167-175.

[3]. X. Lao, Q. Tang, A. Shen, and Q. Zhang, PMSM Sensorless Control by injecting HF pulsating carrier signal into estimated fixed frequency rotating reference frame, IEEE Transactions on industrial electronics 2016, 63(4), 2294-2303.

[4]. Y. Li, X. Wang, and W. Hu, Sensorless control of PMSM based on low-frequency current signal injection in the direct axis at low zero speed. Applied Mechanics Material, 2011, 143(4) 103-107.

[5]. Z.M.S. El-Barbary, Single to three phases induction motor sensorless drive system. Alexandria Engineering Journal, 2012, 51(6) 77-83

[6]. M. Pucci, and M. Cirrincione, Neural MPPT control of wind generators with induction machines without speed sensors. IEEE Transaction on Industrial Electronics. 2011, 58 (1), 37-47.

[7]. I. Zheng, J.E. Fletcher, B.W. Williams, and X. He, A novel direct torque control scheme for a sensorless five phase induction motor drive. IEEE Transaction on Industrial Electronic, 2011, 58(2), 503-518.

[8]. I. Vicente, A. Endenalio, X. Garin, and M. Brown. Comparative study of stabilizing methods for adaptive speed sensorless full-order observers with stator resistance estimation. IET control theory and application. 2010, 4(6), 993-1004.

[9]. T. Orlowska-Kowalska, and M. Dybkowski. Stator-current based MRAS estimator for a wide range speed-sensorless induction motor drive. IEEE Transaction on Industrial Electronic, 2010, 57(4), 1296-1308.

[10]. G. Zizbao, X. Guofei, P. Ming, and D. Songyi, Sensorless Drive of Direct Torque Controlled PMSMs based on Robust Extended Kalman Filter, Proceedings of the 35th Chinese control conference, Chenglu China, 27-29 July, 2016, 4711-4716.

[11]. S. Bolognani, L. Tubiama, and M. Zigliotto, Extended Kalman Filter tuning in sensorless PMSM drives. IEEE Transactions on Industrial Applications, 2003, 39(6), 1741-1747.

[12]. K. Zowiriski, H. Janisewski, and R. Musnynski, Unscented Extended Kalman Filters Study For Sensorless Control of PM Synchronous Motors with Load Torque Estimation Bulletin of the Polish Academy of Sciences Technical Sciences, 2013, 61(4) 793-801.

[13]. T. Bernardes, V. Montagner, H. Grumllingand H. Pinheiro, Discrete-Time Sliding mode observer for Sensorless Vector Control of Permanent Magnet Synchronous Machine, IEEE Transaction on Industrial Electronics, 2014, 61(4), 1679-1691.

[14]. Z. Chen, L. Wang, and X. Liu, Sensorless direct Torque Control of PMSM using Unscented Kalman Filter IFAC proceedings, 2011, 44(1), 4380-4385.

[15]. Lu Lin-Yu, Y. Tzu-Wei, ChuChia-chi, Back-Emf Based Model-Reference Adaptive Sensorless Control for Grid connected DFIG's IEEE 978-1-4799-1303-913, 2013.

[16]. A.Y.E. Lesan, M.I. Doumbia, and P. Sicard, Comparative Study of Speed estimation techniques for sensorless vector control of induction machine IECON 2012-38th Annual conference on IEEE Industrial Electronics Society, Montreal QC4298-4303, 2012.

[17]. D. Rajalakshimi, Analysis of speed estimation for sensorless induction motor using model based artificial intelligent estimation techniques proceedings of the International conference on soft computing system. Springer, India, 2016, 765-770.

[18]. V. Verma, M.J. Hossain, T. Saba, and C. Chakraborty, Performance of MRAS Based Speed Estimators for Grid Connected Doubly Fed Induction Machines during Voltage Dips. IEEE 978-1-4673-2729-912, 2012.

[19]. Y. Zhao, W. Qiao, and L. Wu, Model Reference Adaptive system Based speed Estimators for sensorless control of interior permanent magnet synchronous machines in proceedings of IEEE Transportaion Electrification conference Expo (ITEC) Detroit USA, 16-19 June, 2013, 1-6.

[20]. A. Samat, D. Ishak, P.Saedin, andS. Iqbal, Speed-Sensorless Control of Parallel-connected PMSM Fed by A Single Inverter Using MRAS IEEE International Power Engineering Optimization conference. Melaka, Malaysia June, 2012, 35-39.

[21]. B.K. Bose, Modern Power Electronics and A.C. Drives. Eagles Woods Cliffs Prentice Hall, P.T.R Upper Saddle River 2012.

[22]. J.J. Listwan, Analysis of Fault States in drive systems with multi-phase induction motors. Archives of Electrical Engineering. 2019, 68(4), 817-830

[23]. H. Chaabane, K.D. Eddine, and C. Salim, Sensorless backstepping control using a Luenberger Observer for double-star induction motor. Archives of Electrical Engineering, 2020, 69(1), 101-116.

[24]. R.A.K. Aswad, and B.M.H. Jassim, Open-circuit fault diagnosis in three-phase induction motor using model-based technique. Archives of Electrical Engineering, 2020, 69(4), 815-827.

[25]. M. Dybkowski, and K. A Klumkowski, Fault tolerant control structure for an induction motor drive system. Automatika, 2016, 57(3), 638-647.

[26]. V. Vasic, S.N. Vukosavic, and E. Levi, A Stator resistance estimating scheme for speed sensorless motor flux oriented induction motor drives. 2003, 18(4), 476-483.

[27]. J. Listwan, and K. Pienkowski, Field-oriented control of five-phase induction motor with open-end stator winding. Archives of Electrical Engineering. 2016, 65(3), 395-410.